# Grain growth, stress, and impurities in electroplated copper

S.H. Brongersma
*IMEC, Kapeldreef 75, B-3001 Leuven, Belgium*

E. Kerr
*IMEC, Kapeldreef 75, B-3001 Leuven, Belgium, and Science of Materials, Trinity College, Dublin, Ireland*

I. Vervoort
*IMEC, Kapeldreef 75, B-3001 Leuven, Belgium*

A. Saerens
*Department of Metallurgy and Materials Engineering, K.U.-Leuven, B-3001 Leuven, Belgium*

K. Maex
*IMEC, Kapeldreef 75, B-3001 Leuven, Belgium, and Electrical Engineering Department, K.U.-Leuven, B-3001 Leuven, Belgium*

(Received 5 February 2000; accepted 21 December 2001)

The widely observed secondary grain growth in electroplated Copper layers is shown to be incomplete after the sheet resistance and stress of the layer appear to have stabilized. Instead the layer is in an intermediate state with a grain size distribution that depends on the plating conditions. Further extensive annealing at high temperatures results in an additional considerable enlargement of the grain structure, accompanied by an additional decrease of the sheet resistance and desorption of impurities that were incorporated during plating.

## I. INTRODUCTION

The introduction of copper as the new interconnect material of choice has necessitated a firm understanding of the physical properties of this material in both thin films and narrow structures (trenches). It quickly became clear that electroplating provided the most advantageous means of deposition in terms of cost and, equally important, filling of trenches without voids.[1] The latter was achieved through the use of several additives in the electroplating bath that result in an accelerated growth from the bottom of the trench upward.[2] Although the use of these additives facilitates an easy and effective way to fill high aspect ratio structures, it also induces two less desirable phenomena. Firstly, the accelerated 'bottom-up' growth tends to overshoot, producing large hillocks over patterned areas.[3] Secondly, one of the additives (known as brightener) also causes a reduction in as-deposited grain size to a subcritical value. This induces a phenomenon known as self-annealing, in which secondary grain growth occurs at room temperature over a period of days or weeks, accompanied by stress changes and a 20% decrease in sheet resistance $R_S$.

In our early work we showed that sheet resistance and stress are in fact due to two different phenomena.[4] Sheet resistance changes in copper thin films have been shown to relate to changes in grain structure, while the as-deposited stress varies with impurity concentration. Focused ion beam microscopy (FIB) shows a close correlation between secondary grain growth and the decrease of $R_S$. Some discrepancies between the two have been reported,[5] but we believe that these are due to the fact that $R_S$ is sensitive to both normal and secondary growth, while FIB reflects the latter only.

Through the brightener concentration [B], we could vary the as-deposited stress $\sigma_0$ over a range of tensile values ($80 > \sigma_0 > 30$ MPa).[6] Because all of these stress levels reduce to near-zero values during self-annealing, grain boundary volume elimination could be ruled out as the main cause for stress changes as one would expect an increase of tensile stress in this case. It should be noted, however, that other authors[7] have found convincing evidence of layer contraction when using different additives in the plating chemistry. Apparently these additives play a critical role in the behavior of the deposited material.

Later we showed that there is a limit $a_0$ to the final grain size during secondary grain growth that can be obtained.[8] This was attributed to an accumulation of impurities in the moving grain boundaries of the growing grains. When this concentration reaches a critical limit, further grain boundary motion is inhibited.

Below we will present data that not only confirm the results mentioned above but also show how the various pieces fit into a more complete description of the intimately interconnected changes in grain size, stress, and sheet resistance.

 

## II. EXPERIMENTAL

For this study we used 8-in. Si(100) wafers with a native oxide. First a 30-nm TaN layer and a 150-nm Cu seed layer were plasma vapor deposited (PVD). The TaN layer acted as a barrier for copper diffusion into the silicon oxide and additionally caused better adhesion of the copper. The PVD copper layer was used as an electric contact during subsequent electroplating. Then a Semitool Inc. (Kalispell, MT) electroplating chamber with the Nanoplate2001™ chemistry from Shipley Inc. (San Diego, CA) was used to deposit a series of Cu layers under varying conditions. The behavior of these layers of interest depended strongly on the proprietary additives that were present in the plating bath. These included a brightener (e.g., dithiosulfonzuur) and suppressor (e.g., polypropyleneglycol) designed to improve the filling of deep trenches.

The concentration of brightener [B] was determined using a cyclic voltametric stripping technique. It is typically a sulfuric compound that enhances nucleation of new grains during deposition, thereby reducing the as-deposited grain size. As the grain size decreases, surface roughness decreases and more reflective layers are obtained (hence the name). The suppressor is meant to inhibit growth and is a large organic compound that is active on the wafer surface and very wide structures only (>5 μm). Sheet resistance measurements with a KLA-Tencor RS75 (San José, CA) were used to monitor changes during the self-anneal and reflect the average of 49 points distributed evenly over the wafer surface. Experiments at elevated temperatures were performed in a Sum 11k probe station from Cascade in combination with a HP 4156. Stress in the films was determined by measuring changes in curvature of the wafers using a KLA-Tencor Flexus and the 900TC multiprobe system from Frontier Semiconductor (FSM, San José, CA). This last system was complemented by low energy ion scattering (LEIS) measurements at Calipso (Eindhoven, The Netherlands) giving the elemental surface concentration using 3 keV $^4$He scattering. Both of these systems also measure desorption from the layer using a residual gas analyzer. Full polar scans were performed with x-ray diffraction measurements to determine changes in the crystallographic composition of the layers.

## III. RESULTS

Figure 1 shows the decrease of normalized sheet resistance over time at room temperature. As reported extensively in literature there is a strong dependence of the halftime $t_R$ of this transition on layer thickness, but the total decrease is the same for all layers. The change in $t_R$ has been shown to be largely due to a change in 'nucleation sites' per unit area with increasing layer thickness as these sites are proportional to layer volume.[8,9] The use of the term "nucleation" is somewhat ambiguous here as it is used to indicate the onset of growth for a secondary grain.

For layers deposited with different plating currents $I_P$ the situation is somewhat different (Fig. 2). Not only is the $t_R$ different for the various $I_P$, the magnitude of the decrease also changes. Because the impurity concentration is higher for lower $I_P$, grains will grow to a smaller final grain size $a_0$. This not only results in a higher final $R_S$ but also a higher $t_R$ because more nucleation events are needed to transform the entire matrix,[8] and each grain grows slower because impurities hamper grain boundary motion.[10] However, because of the existence of a limiting grain size, we obtained roughly similar grain size distributions for thick and thin films despite the lower number of nucleation sites per unit area. Without such a limit one would expect the few remaining sites for a thin film to grow to much larger sizes before growing into one another.

We now turn to the stress changes observed during the decrease in sheet resistance illustrated in Fig. 2. Figure 3 shows the as-deposited stress $\sigma_0$ and the final stress $\sigma_F$

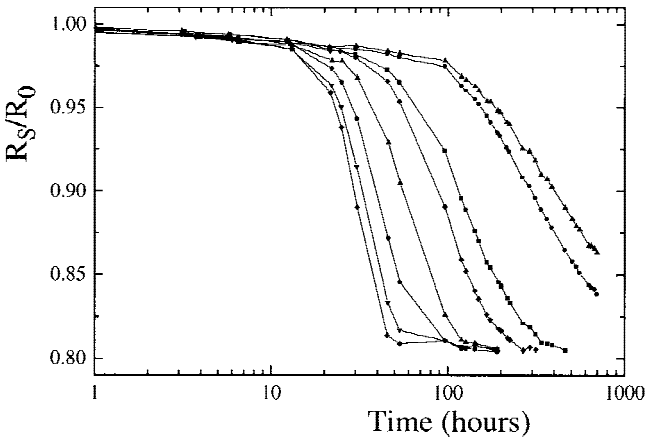


FIG. 1. $R_S(t)$ for layers with a thickness of 3.15, 2.15, 1.45, 1.15, 0.90, 0.75, 0.65, and 0.55 μm from left to right, respectively. These values include the 150-nm seed layer, and the layers were plated at $I_P = 6$ A.

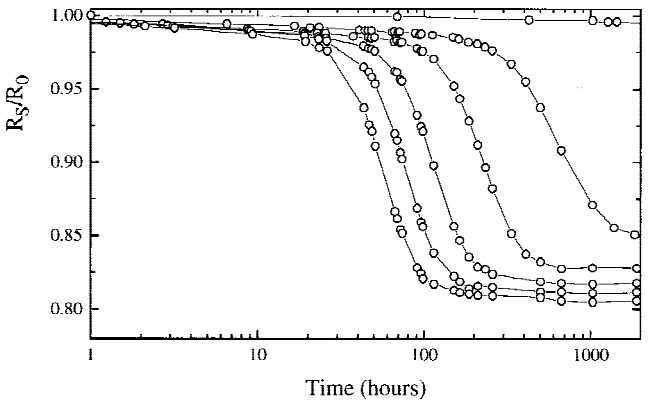


FIG. 2. $R_S(t)$ for layers plated at 6.0, 4.5, 3.0, 1.5, 0.75, and 0.3 A from left to right, respectively. The layer thickness was 1.15 μm.

for several values of $I_P$. It shows that the initial stress can be varied over a wide range of both tensile and compressive values with a crossover at $I_P = 1.0$ A, while $\sigma_F$ depends only slightly on $I_P$.

It should be noted that the impurity incorporation rate varies with aging of the plating bath, as brightener has to be added frequently to maintain its composition while breakdown products remain in the solution. Thus, while a cyclic voltametric stripping measurement indicates identical additive concentrations, there may be a bath aging effect on stress levels in the deposited layers. With a typical plating bath lifespan of 2–3 months, experiments made several weeks apart should thus be compared with care, as the curve in Fig. 3 will shift over time.

The fact that the stress reduces in absolute terms for both initial tensile and compressive stress clearly illustrates that stress changes are indeed not governed by grain boundary volume elimination. For high plating currents, where fewer impurities are incorporated, the stress converges to approximately 80 MPa. This value is consistent with literature[11] on electroplating of metals.

As published previously,[6] Fig. 4 shows the dependence of $\sigma_0$ on brightener concentration extrapolated back to the same value of approximately 80 MPa for [B] = 0. It shows a compressive addition to $\sigma_0$ (decreasing tensile stress) for increasing [B] that can be understood by a higher incorporation of impurities. When looking at the grain structure as a function of [B] and $I_P$ we see that, for both very low [B] and very low $I_P$, a similar surface roughening and grain structure is observed while the stress trends are opposite (most tensile for low [B] and most compressive for low $I_P$). This once again indicates that the stress is determined by impurity incorporation and not by changes in grain structure.

A combined measurement of stress, desorption, and reflectivity as a function of temperature was made at Frontier Semiconductor on a layer plated at 1.5 A (Fig. 5).

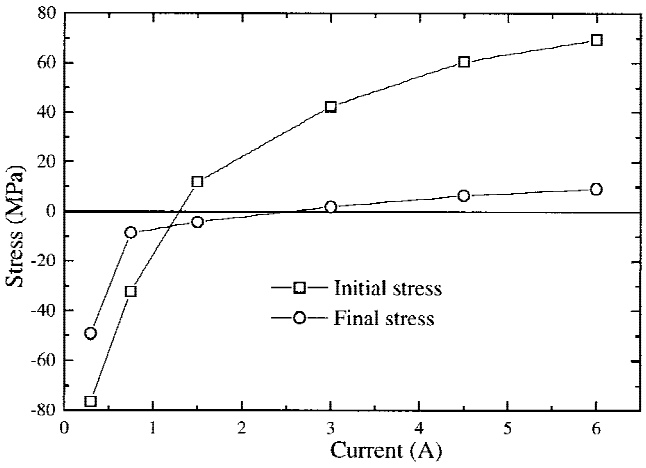


FIG. 3. As-deposited stress and the final stress to which it decreases during self-annealing as a function of plating current. The layer plated with the lowest current was not fully recrystallized.

It shows a significant desorption of carbon-related species (CH, CO, etc.) accompanied by a small stress relaxation at approximately 100 °C, confirming our understanding of a compressive component to the stress due to impurity incorporation. A further desorption and a change in reflectivity are observed at higher temperatures. This is related to a cleaning of the surface, contaminated because of the unavoidable organic adsorption to metal surfaces in air, through the significant hydrogen desorption discussed below.

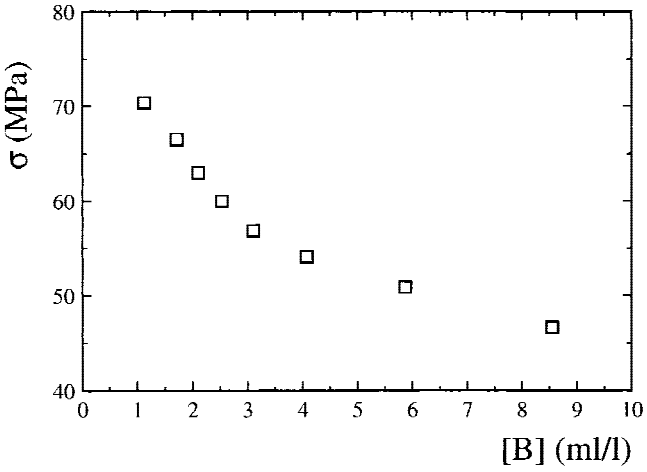


FIG. 4. As-deposited stress as a function of brightener concentration in the plating bath.

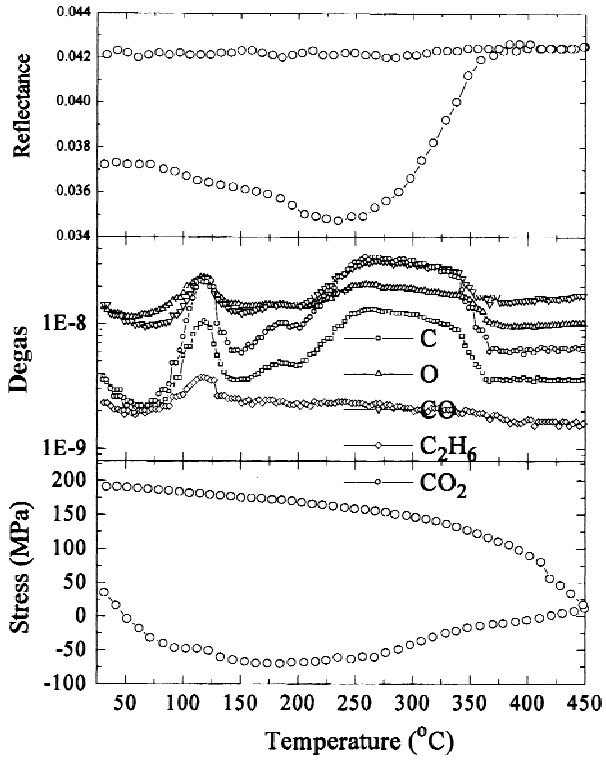


FIG. 5. Stress, desorption, and reflectivity of a copper layer plated at 1.5 A during a thermal cycle at 5 °C/min.

Because of aging, and the resulting partial self-anneal, during transport, the stress relaxation represents only part of the changes that occur during a full recrystallization. When thermally cycling a series of copper layers in house with a range of different $\sigma_0$ at 3 °C/min just after plating, we obtain the curves depicted in Fig. 6, showing a much more pronounced effect. Interestingly, the stress change during relaxation is proportional to the stress built in to the layer during deposition, resulting in a collapse of the curves for $T > 120$ °C. Thus all layers are in a similar stress state just after the stress relaxation. However, the variations in stress after the full cycle to 400 °C indicate that there still are some differences between the layers.

Further evidence of impurity migration to the surface was found in low-energy ion scattering measurements that monitor the elemental concentrations on the surface using 3 keV $^4$He scattering. To start with a clean surface without heating the sample or needing a plasma treatment, a highly reactive atomic oxygen beam was used in the pre-treatment chamber of the Calipso setup. Figure 7 shows carbon and very small amounts of nitrogen appearing at the surface around 80 °C and disappearing again before reaching 150 °C.

The next step is to check how the sheet resistance behaves during the observed desorption and the accompanying stress changes. While using a ramp rate of 5 °C/min we found that the sheet resistance also exhibits large changes in the same temperature range as the stress. The initial part of the curve in Fig. 8, depicting $R_S$ versus temperature, is fairly straight although, when using a ruler, the behavior is clearly nonlinear. As a comparison a PVD copper layer is shown that, as expected according to Matthiessen's rule, is perfectly linear. At approximately 100 °C $R_S$ decreases sharply, suggesting that changes should also be seen in grain structure. The three focused ion beam images show that grain growth does indeed occur simultaneously. However, the deviation from a straight line at low temperatures already suggests that there is nothing special about the temperature at which the transition occurs, but rather it is the temperature at which the transition can be accomplished within a reasonable timeframe at this particular ramp rate. The

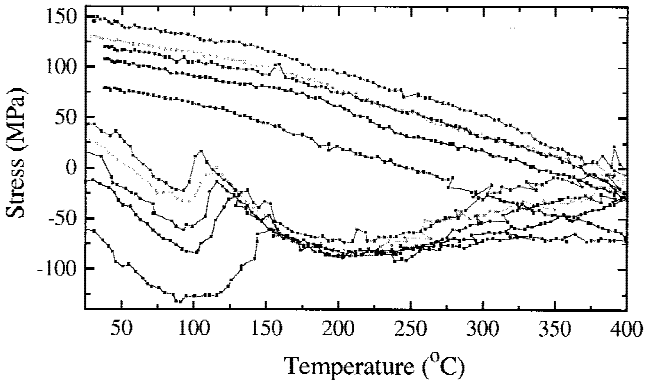


FIG. 6. Thermal cycles to 400 °C as obtained at 3 °C/min for five layers with a different initial stress obtained by varying the plating current.

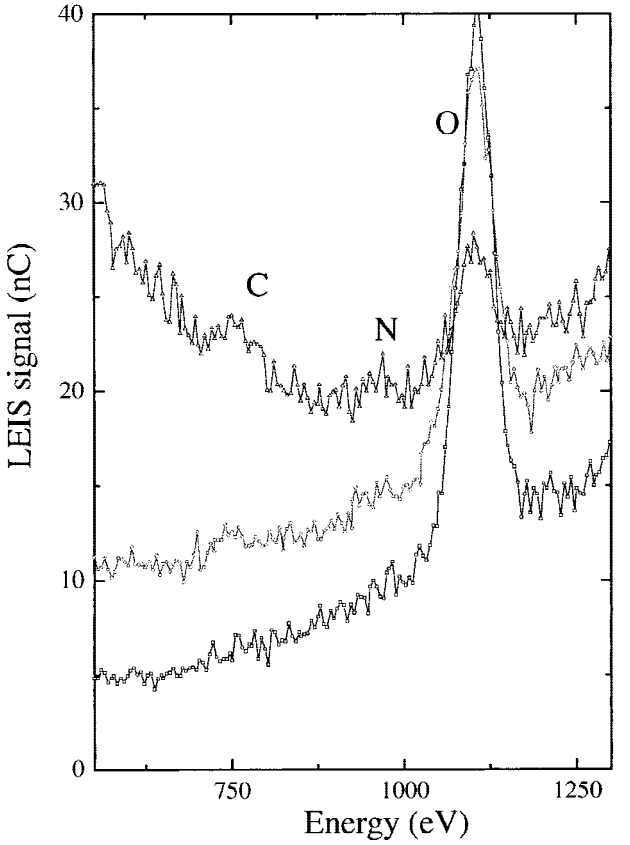


FIG. 7. LEIS spectrum obtained for 3 keV $^4$He scattering at 85, 120, and 150 °C from top to bottom, respectively. As opposed to the C and N peaks the O peak was already there at 60 °C and is most likely mainly due to a native oxide.

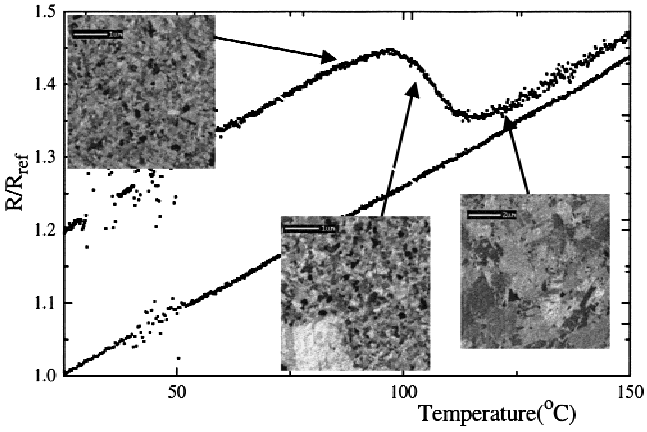


FIG. 8. Thermal cycle measured at 5 °C/min for a PVD Cu layer (lower curve) and an electroplated layer (upper curve) of 1.15 μm plated at 3.0 A. The three FIB images illustrate how the grain structure changes during the transition. Both curves are normalized to their sheet resistance after full annealing.

difference between the two curves at elevated temperatures indicates that grain growth is not completed once the main drop in sheet resistance has occurred.

Figure 9 shows further evidence that this phenomenon is simply thermally activated and just accelerates for higher temperatures. The sheet resistance versus time is depicted at different temperatures, and clearly the curves are simply shifted in time. The difference in magnitude of the decrease in $R_S$ for the four curves is due to the normalization. As the total change is identical in absolute terms, the higher $R_S$ for higher $T$ makes the decrease look smaller. The inset shows $\ln(t_R)$ versus $10^3/T$, and from the slope of this linear dependence an activation energy of 0.92 eV was derived.

Despite the linear dependence of the inset in Fig. 9, there is a significant crystallographic difference between the layers annealed at different temperatures $T_A$. The large left part of Fig. 10 shows how the volume fractions of the (111) and (200) orientations after annealing depend on $T_A$. While the (200) concentration decreases slightly, the (111) volume fraction increases significantly with temperature. As the stress is always below the threshold biaxial stress for preferential (200) growth, it is no surprise that the volume fraction for this orientation does not increase. In fact, the increase in (111) affects the rest of the matrix [both (200) and randomly oriented grains] in a homogeneous way.

So far we have looked at the behavior of copper layers at relatively low temperatures. Although all layers show similar remarkable changes in their physical properties there are many subtle differences suggesting that the state of these layers is not the same. To check the true stability of these layers a sample plated at $I_P = 0.75$ A, for which $R_S$ reduced by only 12% before stabilizing, was heated to 400 °C and kept there for 20 h. This resulted in an additional decrease to a total of 20%, and Fig. 11 shows the resulting grain structure after this treatment. Thus, even though stress and sheet resistance appeared stable after the transition, substantial further grain growth was observed. Also, the layers plated using different $I_P$s, which had a different sheet resistance after the main decrease was over (Fig. 2), all go down to the full 20% after this extensive high-temperature anneal. This means that, for example, a layer plated with a lower current decreases less during the initial grain growth at relatively low temperatures and consequently decreases more during this long high-temperature anneal. Deviations from this behavior are expected to occur for very low [B], where grains already grow highly faceted and the initial sheet resistance will also not be as high.

The low energy ion scattering spectrum shown in Fig. 12 demonstrates that there is also an additional migration of impurities to the surface. Sulfur is detected for temperatures as low as 150 °C, but the surface concentration increases slightly towards 400 °C. As sulfur was not detected during the low-temperature recrystallization but now starts to desorb when grain growth continues, this element may in fact be responsible for stabilizing the

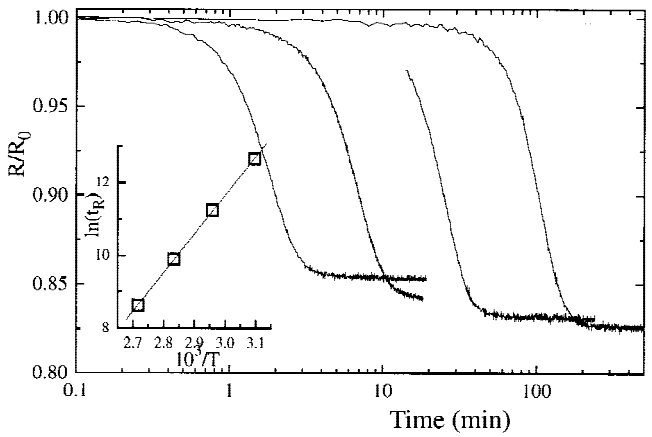


FIG. 9. Normalized sheet resistance versus time for $I_P = 3.0$ A as measured at 50, 65, 80, and 95 °C from right to left. The slope of the curve in the Arrhenius plot gives an activation energy of 0.92 eV.

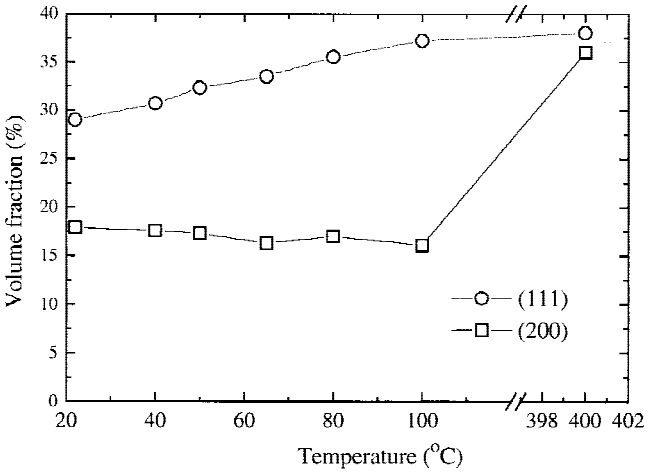


FIG. 10. Volume fractions for the (111) and (200) orientations as a function of annealing temperature.

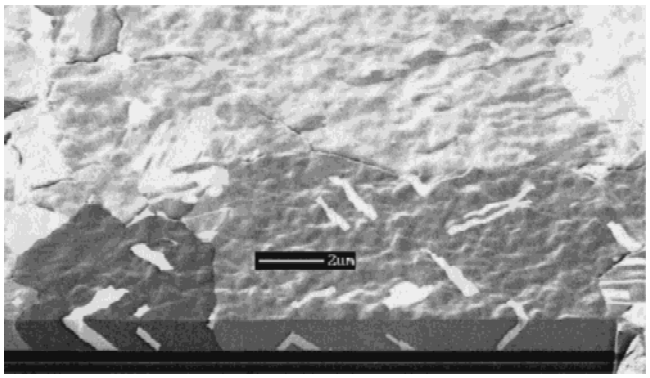


FIG. 11. Combined cross-sectional and surface FIB image of the grains after an anneal at 400 °C

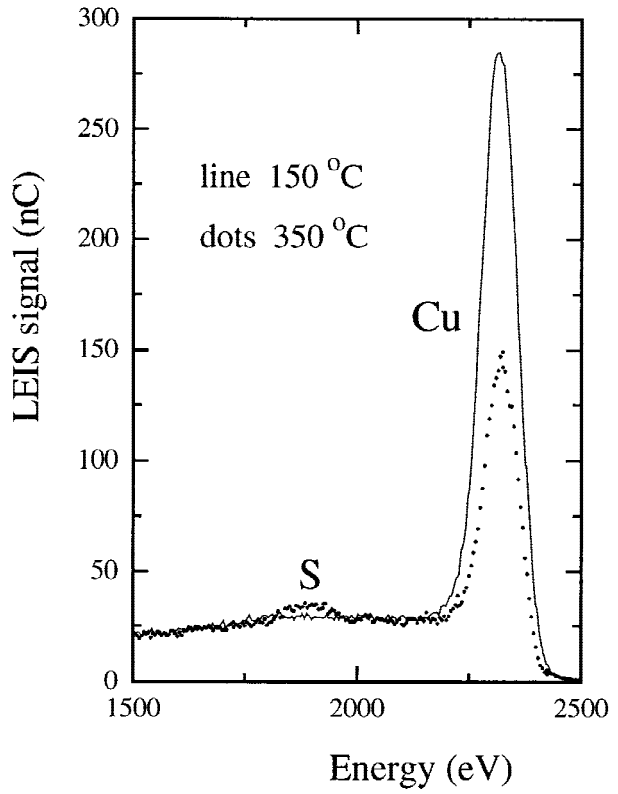


FIG. 12. LEIS signal at 150 and 350 °C showing the migration of sulfur to the surface. The decrease in Cu signal is mainly due to hydrogen coverage.

grain structure. The process is accompanied by significant grooving of the surface as seen in Fig. 11, suggesting that some reduction in volume has now occurred. This is also indicated by the sudden increase of the stress driven (200) volume fraction to 38% as shown in Fig. 8, which apparently does not influence the already established (111) volume fraction.

Finally it should be noted that large amounts of hydrogen come out of the sample and are believed to be instrumental in removing the impurities from the surface. The estimated total of approximately 36 monolayers escaping at elevated temperatures is also more than enough to saturate all existing grain boundaries and stabilize the structure. This was detected in the low-energy ion scattering apparatus using a residual gas analyzer and substantiated by a simultaneous reduction in the Cu signal. As the equipment used here is only sensitive to the outermost atomic layer of the sample and no changes were seen for other elements, the observed decrease can only be explained by hydrogen coverage of the surface. Moreover, after cooling the sample, a very low energy sputtering quickly restores the Cu peak. As the temperature is increased from 200 °C, with approximately 25% of the surface covered by O and H, to 400 °C the Cu peak increases to close to 100%. Thus, the sample surface is cleaned by hydrogen escaping from the layer, clarifying why the reflectivity in Fig. 5 suddenly increases. This also clarifies why plasma vapor deposited Cu layers need a hydrogen plasma to be cleaned while this is not necessary for our electroplated layers.

## IV. DISCUSSION

The behavior of stress, sheet resistance, and grain structure described above can be explained consistently within a model that depends critically on the impurities incorporated in the layer during plating.

The limiting value of 80 MPa is typical for electroplated films because of their rough grains,[12] caused by local blocking of growth by the addition agents. Films are prevented from collapsing as much during deposition as, for example, PVD films, because the contraction of the film ends when grain extremities touch.[12] As a result, there will be some open volume in the boundaries, opening the potential for grain boundary volume elimination and tensile stress buildup. Impurities can be incorporated in both the open volume and the bulk of the grains. Clearly the size of such a volume will help determine how large the influence on the overall stress of an incorporated atom will be. It has been suggested previously for nickel electrodeposits that the voids can fill with hydrogen and cause an expansion leading to a compressive stress.[13] Furthermore, for example, carbon and hydrogen can both occupy interstitial sites in the copper face-centered-cubic lattice of the grains themselves, providing another potential stress source.

During grain growth, the moving boundaries will push all impurities into the boundaries, as was nicely shown by Hau-Riege and Thompson.[14] The limited volume of these boundaries will cause diffusion of the surplus impurities out to the surface, resulting in the observed desorption of carbon and other elements. It should be noted that, even though the original rough grains are now absorbed into the large secondary grains, no increase in tensile stress due to the annihilation of grain boundary volume is observed. This indicates that the volume that was originally present can be compensated by the impurities that remain in the film. This then has to be the hydrogen and sulfur observed in the low energy ion scattering measurements at elevated temperatures.

Thus, the main decrease in sheet resistance observed throughout the literature is accompanied by a cleansing of the bulk of the material, leaving specific impurities in the boundaries only. The activation energy of 0.92 eV was, amongst others, also found by Gupta[15] and attributed to grain boundary self-diffusion. Hau-Riege and Thompson[14] suggested that, even though normal grain growth is impaired by impurities, impurity rejection might in fact contribute to the energy driving secondary grain growth.

We would now like to recollect our earlier work on the existence of a limiting grain size to which grains grow,[8] which was used to explain the observed Avrami coefficients and fit the measured sheet resistance changes with great accuracy. In this model, a higher concentration of impurities, as can be obtained by using a lower plating current, results in a smaller final grain size as a critical concentration in the boundaries is reached for a smaller grain diameter. The eventual inhibition of grain boundary motion and the grain size at which this occurs must now be concluded to be due to the amount of sulfur and/or hydrogen incorporated in the material as carbon does not accumulate in the boundary.

This then explains the behavior observed in Fig. 2 where both the time needed for the self-anneal and the final sheet resistance depend on plating current. The higher impurity concentration obtained for lower current results in a smaller grain size, and more grain boundaries and smaller grains will clearly result in a higher sheet resistance.[9] Furthermore, for a smaller final size of the secondary grains, more of these grains will be needed to transform the entire matrix. It is this increase in the number of required nucleation events that explains the large change in time. Interestingly there is also still a dependence of the final stress on plating current (Fig. 3), which can also be explained by the difference in grain size. The larger number of impurities present in the larger total grain boundary volume for a matrix of smaller grains will give a small compressive contribution to the stress. However, the magnitude of this stress is small compared to the values seen just after plating because the grains themselves have been purified.

This brings us to the phenomena described above for higher temperature anneals. These clearly show that, even though both stress and sheet resistance seem to have stabilized, there are still impurities in the layer and the sheet resistance has not dropped to its bulk value yet due to the still fairly small grain sizes. An additional high-temperature anneal shows that this is indeed the case as evidenced by a further decrease in sheet resistance accompanied by substantial grain growth. The migration of sulfur to the surface at these higher temperatures confirms that there still were impurities present in the layer. The extensive grooving of the boundaries can be understood in terms of a reduction in volume because of a true cleansing of the layer, resulting in tensile stress buildup and subsequently a relaxation of the layer through grain boundary diffusion from the surface as described by Thouless *et al.*[16] This also explains the substantial increase of the stress driven (200) orientation.

The exact behavior of hydrogen in these layers is still under investigation. It is clearly indispensable in helping the desorption of other incorporated impurities, but it was somewhat surprising to still see significant desorption of hydrogen at elevated temperatures. Even though hydrogen is more likely to remain bonded within the copper layer than carbon, the desorption continues to temperatures above those expected for hydrogen in single-crystal copper. This may be due to specific bonding energies in the grain boundaries, surface roughness, or perhaps a bonding to the sulfur atoms that are still present. In fact, whether it is truly sulfur that stabilizes the grain structure after the first phase in the recrystallization or whether hydrogen is involved here as well is unclear.

## V. GENERAL COMPARISON

Over the last two years many apparently conflicting results and interpretations have been published. Clearly these are in part due to the differences between various plating chemistries and other processing parameters used in the industry. Here we will discuss how slight variations in the effects of the additives used can account for some of the confusion.

To start, we ourselves in fact used a different chemistry (Nanoplate 2000$^{TM}$) initially and obtained very different results as compared to our present data. It surprisingly resulted in a substantial difference between time scales of stress release and sheet resistance changes, which led us to the first evidence that stress changes are due to desorption of impurities. Additionally the shape of the curves was very different with the stress reducing almost linearly from $t = 0$, as opposed to the plateau seen in Fig. 2. This suggests a very different structure of the deposit resulting in easy diffusion of impurities through the material, as evidenced by rapid sulfur desorption at room temperature, without the need of growing grains to push them. Unfortunately this plating chemistry is no longer available, and the behavior has not been reported elsewhere. Quite different stress behavior may be expected whe, for example, the impurities are incorporated preferentially in the grain boundaries. Clearly the influence of impurities in the fairly open grain boundary structure will not be the same as an interstitial in the grains themselves. This would most likely result in a smaller dependence of $\sigma_0$ on $I_P$ than presented here, as has been widely observed, but further experiments will be needed to clarify the relative importance of the various incorporation sites in causing the strong dependence shown in Fig. 3.

A further change in behavior may be expected for low concentrations of impurities, or even different ratios of the impurity concentrations. The large grain boundary volume eliminated during the first phase of the recrystallization must somehow be compensated for by the remaining impurities to prevent contraction of the film. This will not be, for instance, the case when the easily migrating carbon is the main impurity causing stress buildup and preferential (200) growth to occur already

during the first phase recrystallization. This is indeed seen by Lee *et al.*,[7] while in our case this does not occur until the extensive anneal at high temperatures.

A low sulfur incorporation could also prevent the growth stagnation from ever occurring, resulting in a large influence on the dynamics of growth and consequently on the observed Avrami coefficient.

However, despite all of the above, it should be noted that no contradictory evidence has ever been published for the dependence of $t_R$ on $I_P$.[7,10] Apparently electroplating consistently results in at least some incorporation of the additives, and thus a higher $t_R$ is always found for lower $I_P$ as the resulting higher impurity concentrations slow down transformation of the material.

## VI. CONCLUSIONS

Our copper layers start in a stress state determined by an intrinsic tensile contribution of approximately 80 MPa and a compressive term resulting from impurity incorporation. The small as-deposited grain structure goes through a recrystallization that essentially consists of two different phases. The first phase is the generally observed decrease in sheet resistance where secondary grains push impurities into the grain boundaries and out to the surface as they grow. When the structure stabilizes it is only in an intermediate state where the grains themselves are purified and the grain size depends on the as-deposited concentration of less mobile impurities (and thus on plating current). From desorption data it follows that mainly carbon-related compounds (e.g., CO, $C_2H_6$, $CO_2$) come to the surface during this initial phase while hydrogen and sulfur remain in the material.

A second phase is observed during a further anneal at 400 °C, causing additional desorption and significant grain growth, resulting in a further drop in sheet resistance. Only after this extensive high-temperature anneal do all layers reach a similar low resistivity and purified state. The accompanying contraction of the layer results in substantial stress-driven (200) growth.

Not only does this model explain the details of grain growth, stress, and sheet resistance for our layers, it also shows how slight changes in concentrations and/or behavior and of the additives can lead to very different observations. These include an as-deposited stress that does not depend on plating current and a buildup of tensile stress during recrystallization.

Additionally, it implies that any low-temperature anneal terminated when the sheet resistance appears to have stabilized will not give the lowest resistivity possible and will consequently lower interconnect performance.

## REFERENCES


1. D.C. Edelstein, Proc. SPIE Conf, Multilevel Interconnect Technol. II **3508,** 8 (1998).
2. M.E. Gross, K. Takahashi, C. Lingk, T. Ritzdorf, and K. Gibbons, Conf. Proc. ULSI XIV 1999, p. 51.
3. E. Richard, I. Vervoort, S.H. Brongersma, H. Bender, G. Beyer, R. Palmans, S. Lagrange, and K. Maex, Conf. Proc. Advanced Metallization Conference 1999, edited by Mihal E. Gross (Mater. Res. Soc.).
4. S.H. Brongersma, I. Vervoort, M. Judelewicz, H. Bender, T. Conard, W. Vandervorst, G. Beyer, E. Richard, R. Palmans, S. Lagrange, and K. Maex, Proc. of IITC-1999, p. 290.
5. D. Walther, M.E. Gross, K. Evans-Lutterodt, W.L. Brown, M. Oh, S. Merchant, and P. Naresh, in *Materials, Technology, and Reliability for Advanced Interconnects and Low-k Dielectrics*, edited by G.S. Oehrlein, K. Maex, Y-C. Joo, S. Ogawa, and J.T. Wetzel (Mat. Res. Soc. Proc. **612,** Warrendale, PA, 2001), p. D10.1.1.
6. S.H. Brongersma, E. Kerr, I. Vervoort, E. Richard, and K. Maex, Accepted for Conf. Proc. Advanced Metallization Conference 2000, edited by D. Edelstein, G. Dixit, Y. Yasuda, and T. Ohba (Mat. Res. Soc.), p. 161.
7. H. Lee, S.D. Lopatin, and S.S. Wong, Proc. of the IITC-2000, p. 114.
8. S.H. Brongersma, I. Vervoort, E. Richard, and K. Maex, Proc. of the IITC-2000, p. 31.
9. J.M.E. Harper, C. Cabral, Jr., P.C. Andricacos, L. Gignac, I.C. Noyan, K.P. Rodbell, and C.K. Hu, J. Appl. Phys. **86,** 2516 (1999).
10. M.A. Gribelyuk, S.G. Malhotra, P.S. Locke, P. DeHaven, J. Fluegel, C. Parks, A.H. Simon, and R. Murphy, Proc. of the IITC-2000, p. 188.
11. E.S. Machlin, *Materials Science in Microelectronics*, Chapter VI, p. 157.
12. K. Raghunathan and R. Weil, Surf. Technol. **10,** 331 (1980).
13. K. Sheppard and R. Weil, in *Thin Films: The Relationship of Structure to Properties*, edited by C.R. Aita and K.S. SpeeHarsha, (Mat. Res. Soc. Symp. Proc. **47**, Pittsburgh, PA, 1985), p. 127.
14. S.P. Hau-Riege and C.V. Thompson, Appl. Phys. Lett. **76,** 309 (2000).
15. D. Gupta, in Mat. Res. Soc. Proc. **337**, 209 (1994).
16. M.D. Thouless, J. Gupta, and J.M.E. Harper, J. Mater. Res. **8,** 1845 (1993).